Supporting Online Material for

In vivo imaging reveals an essential role for neutrophils in Leishmaniasis transmitted by sand flies

Nathan C. Peters[1,2], Jackson G. Egen[1,3], Naglia Secundino[2], Alain Debrabant[4], Nicola Kimblin[2], Shaden Kamhawi[2], Phillip Lawyer[2], Michael P. Fay[5], Ronald N. Germain[3,6], David Sacks[2,6]

[1,6]These authors contributed equally to this work. [2]Laboratory of Parasitic Diseases, [3]Laboratory of Immunology, and [5]Biostatistics Research Branch, National Institute of Allergy and Infectious Diseases, National Institutes of Health, Bethesda, MD, 20892, USA. [4]Division of Emerging and Transfusion Transmitted Diseases, OBRR, CBER, Food and Drug Administration, Bethesda, MD 20892, USA.

Correspondence regarding sand flies and *Leishmania* infection should be addressed to D.L.S. (dsacks@nih.gov)

Correspondence regarding intravital imaging should be addressed to J.G.E. (jegen@niaid.nih.gov)

This PDF file includes:

- Materials and Methods
- Figs. S1 to S7
- References

Other Supporting Online Material for this manuscript includes the following:

- Movies S1 to S14

Supplemental Materials and Methods

Mice

C57BL/6 LYS-eGFP knock-in mice (*1*) were a gift from T. Graf (Albert Einstein University, NY) and C57BL/6 IA^b-eGFP knock-in mice (*2*) were a gift from H. Ploegh (Harvard University, MA). These animals were bred and maintained at Taconic Laboratories through a special contract with the NIAID. CSF1 Receptor-eGFP mice (Jax Stock# 5070) were obtained from Jackson Laboratories. C57BL/6 mice were purchased from Taconic Laboratories. All mice were maintained at the NIAID animal care facility under specific pathogen-free conditions and were used under a study protocol approved by the NIAID Animal Care and Use Committee.

Generation of Leishmania major-RFP

A stable transfected line of *L. major* V1 (MHOM/IL/80/Friedlin) promastigotes expressing a red fluorescent protein was generated as described previously (*3*). Briefly, the DsRed gene was amplified by PCR using the pCMV-DsRed-Express plasmid (BD Biosciences/Clontech) as a template and cloned into the SpeI site of the pKSNEO Leishmania expression plasmid. FV1 promastigotes were transfected with the resulting expression plasmid construct [pKSNEO-DsRed] or the empty control plasmid [pKSNEO] and selected for growth in the presence of 50 µg/ml Geneticin (G418) (Sigma). The resulting parasites are referred to as *L. major*-RFP or *L. major*-NT, respectively. FV1-RFP fluoresces brightly and grows and infects flies and mice normally.

Sand fly feeding and sand fly transmission of L. major

Sand fly transmission of *L. major* infection was performed as described (*3*). Briefly, 2-4 day old *P. duboscqi* female sand flies were infected via artificial feeding through a chick skin membrane on heparinized mouse blood and *L. major* or *L. major*-RFP amastigotes or promastigotes. After 13-19 days, individual flies were transferred to plastic vials covered at one end with nylon mesh. Mice were anesthetized by intraperitoneal injection of 30µl of ketamine/rompin (100mg/ml). Specially designed clamps were used to bring the mesh end of each vial into contact with the ear of an anesthetized mouse, allowing flies inside the vial to feed on the ear skin for a period of 30 minutes to 3 hours in the dark. In some experiments uninfected age-matched flies were also employed and allowed to feed in the same manner as infected flies. The number of flies with blood meals was employed as a means of checking for equivalent exposure to potential transmission by sand fly bite among animals in different treatment groups.

Parasite preparation and needle inoculation

L. major or *L. major*-RFP were grown at 26 °C in medium 199 supplemented with 20% heat-inactivated FCS (Gemini Bio-Products), 100U/ml penicillin, 100µg/ml streptomycin, 2mM L-glutamine, 40mM Hepes, 0.1 mM adenine (in 50mM Hepes), 5mg/ml hemin (in 50 % triethanolamine), and 1mg/ml 6-biotin (M199/S). Infective-stage metacyclic promastigotes of *L. major* were isolated from stationary cultures (4-5 day-old) by negative selection of non-infective forms using peanut agglutinin (PNA, Vector Laboratories Inc). For flow cytometry experiments, mice were infected with the specified number of parasites in the ear dermis by intra-dermal (i.d.) injection using a 29

½ GA needle in a volume of 10µl unless specified otherwise. For imaging experiments, mice received i.d. injections of $1x10^4$ parasites in a volume of 1-2µl.

Processing of tissue

Ear tissue was prepared as previously described (*4*). Briefly, the ventral and dorsal sheets of infected ears were separated, deposited in DMEM containing 100U/ml penicillin, 100µg/ml streptomycin and 0.2mg/ml Liberase CI purified enzyme blend (Roche Diagnostic Corp.), and incubated for 2 hours at 37°C and 5% CO_2. Digested ear sheets were homogenized using the Medicon/Medimachine tissue homogenizer system (Beckton Dickinson). Retromaxillary (ear) lymph nodes were removed, pooled, and mechanically dissociated using tweezers and a syringe plunger. Tissue homogenates were then filtered using a 70µm-pore size Falcon cell strainer (BD Biosciences).

Immunofluorescence Microscopy

Ears were excised, fixed with 4% paraformaldehyde/PBS for 12 hours and dehydrated in 30% sucrose/PBS prior to embedding in OCT or TFM freezing media (Electron Microscopy Sciences). 25µm sections were cut on a CM3050s cryostat (Leica) and adhered to Superfrost Plus slides (VWR). Sections were permeablized and blocked in PBS containing 0.3% Triton X-100 (Sigma) and 10% goat serum (Jackson Immunoresearch) followed by staining with AlexaFluor 647-conjugated anti-F4/80 (clone BM8) (Caltag) and Hoechst 33342 (Invitrogen). Stained slides were mounted with Prolong Gold (Invitrogen) and 3D image stacks were acquired on a LSM 510 confocal

microscope (Carl Zeiss Microimaging). Images are displayed as 2D maximum intensity projections.

Two Photon Intravital Skin Imaging and Image Analysis

Mice were anesthetized using isoflurane (Baxter) as previously described (*5*) and placed in a lateral recumbent position on a custom imaging platform such that the ventral side of the ear pinna rested on a coverslip. A strip of Durapore tape (3M) was placed lightly over the ear pinna and affixed to the imaging platform in order to immobilize the tissue. Care was taken to minimize pressure on the ear. Images were captured towards the anterior half of the ear pinna where hair follicles are sparse. In some experiments, blood vessels were visualized by injecting non-targeted Quantum Dots 705 (QD705) (Invitrogen) i.v. immediately prior to imaging.

Images were acquired using an inverted LSM 510 NLO multiphoton microscope (Carl Zeiss Microimaging) enclosed in a custom-built environmental chamber that was maintained at 32^0C using heated air. This system had been custom fitted with 3 external non-descanned PMT detectors in the reflected light path. Images were acquired using either a 20x/0.8 NA air objective or a 40x/1.1 NA water immersion objective. Fluorescence excitation was provided by a Chamelon XR Ti:Sapphire laser (Coherent) tuned to 920nm for eGFP excitation. In some experiments, collagen fibers in the dermis were visualized by detection of second harmonic signals generated at 460nm. Typical voxel dimensions were 0.9 x 0.9 x 2-3μm using the 20x objective and 0.45 x 0.45 x 1-2μm using the 40x objective. For 4-dimensional data sets, 3-dimensional stacks were captures every 1 minute, unless otherwise specified.

Raw imaging data were processed with Imaris (Biplane) using a Gaussian filter for noise reduction. Automatic 3D object tracking using Imaris Spots was aided with manual corrections to retrieve cell spatial coordinates over time. These data were imported into MatLab (MathWorks) for calculating cell velocities. For dynamic display of imaging data sets, image sequences exported from Imaris were composed in AfterEffects (Adobe) to produce video clips. All images and movies are displayed as 2D maximum intensity projections, unless otherwise stated.

Phenotypic analysis of cells

Mice were sacrificed and single cell suspensions from the ear dermis were obtained as described above. Cells were incubated without fixation with an anti-Fc-γ III/II (CD16/32) receptor Ab (2.4G2, BD Biosciences) in RPMI without phenol red (Gibco) containing 1.0% FCS for 10" followed by incubation for 20" with a combination of 4 or 6 of the following antibodies: FITC-, Per-CP Cy5.5-, PE-Cy7, or APC anti-mouse CD11b (M1/70 BD Biosciences); PE-, Per-CP Cy5.5-, or APC-Cy7 anti-mouse Gr-1 (RB6-8C5, BD Biosciences); FITC-, or PE anti-mouse Ly6G (1A8, BD Biosciences); FITC anti-mouse 7/4 (7/4 Cederlane Laboratories); APC- or PE-Cy7 anti-mouse CD11c (HL3, BD Biosciences); APC anti-mouse F4/80 (BM8, eBioscience), FITC anti-mouse I-A^b (AF6-120.1, BD Biosciences); or Alexafluor-700 anti-mouse MHC II (M5/114.15.2, eBioscience). The isotype controls employed were rat IgG1 (R3-34) and rat IgG2b (A95-1). The data were collected and analyzed using CELLQuest software and a FACScalibur or FacsDIVA software and a FacsCANTO flow cytometer (BD Biosciences). Granulocytes/neutrophils and monocytes from the ear dermis were

identified based on size (forward light scatter) and granularity (side light scatter) and by surface phenotype as indicated in the text and figure legends. Extensive analysis of surface phenotypes of dermal derived cells in relation to FSC and SSC using both linear and log scales was employed to ensure relevant cells were not excluded. To confirm phenotypic analysis by flow cytometry and the determination of the number of parasites per cell, differential cell counts were done by microscopic examination of cytospun preparations of ear cells stained with Diff-Quick solution (Dade Behring).

Adoptive transfer of purified, in-vivo infected, dermal neutrophils

LYS-eGFP mice were inoculated in the ear dermis with $2.5x10^6$ *L. major*-RFP in 10ul. Twelve hours later ear tissue was prepared as described above and infected (RFP^+GFP^{hi}) and uninfected (RFP^-GFP^{hi}) neutrophil populations were purified from dermal tissue using a FACSVantage (BD Biosciences) cell sorter. Sorted populations were washed once and immediately injected into the ear dermis of B6 recipient mice in a volume of 5-10ul. For imaging experiments, sorted populations of neutrophils were injected into the ear dermis of CSF1R-eGFP mice that had been exposed to uninfected sand flies 12 hours earlier. The ratio of live infected neutrophils to free parasites in the remaining volume of the injection syringe was 9.9:1(+/- SD 0.8, n=4). The ratio of live versus dead cells among RFP^+GFP^+ sorted neutrophils in the remaining volume of the injection syringe as determined by trypan blue exclusion following cell sorting was 9.2:1 (+/- SD 4.1, n=8). Prior to sorting, infected neutrophils contained an average of 1.5 parasites per cell (+/- SE 0.28 n=3 separate experiments in which greater then or equal

to 54 neutrophils were counted, median = 1.7), as determined from cytospun whole ear preparations.

Estimation of parasite load

Parasite titrations were performed as previously described (*6*). Tissue homogenates were serially diluted in 96-well flat-bottom microtiter plates containing biphasic medium, prepared using 50µl NNN medium containing 20% of defibrinated rabbit blood and overlaid with 100µl M199/S. The number of viable parasites in each ear was determined from the highest dilution at which promastigotes could be grown out after 7-10 days of incubation at 26°C. In some experiments the number of sort purified infected neutrophils containing at least one viable parasite was determined by serial dilution of a known number of infected neutrophils. Titration of sorted $RFP^{+}CD11b^{hi}Gr\text{-}1^{hi}$ neutrophils from C57Bl/6 mice generated similar results to infected neutrophils sorted based on GFP expression, suggesting the survival of parasites in neutrophils is not a peculiarity of LYS-eGFP mice.

Neutrophil Depletion

Neutrophils were depleted employing a single 0.5mg injection of anti-Gr-1(Ly-6G/C) (RB6-8C5) or control (GL113) IgG antibody, i.p., 16 hours prior to sand fly transmission. Success and specificity of depletions were determined as described in the text.

Detection of spontaneous release of IL-1α and IL-1β

Cells prepared from the ear tissue of sand fly transmitted mice were incubated in RMPI medium supplemented with 10% FCS, 100U/ml penicillin, 100µg/ml streptomycin, and 10mM Hepes, for 48 hours at 37°C and 5% CO_2. Supernatants were subsequently removed and the levels of IL-1α and IL-1β were measured using the Searchlight™ multiplex testing service (Pierce Biotechnology).

Statistical analysis

Parasite loads in the ears of mice transmitted with *L. major* by infected sand fly bite do not follow a Gaussian distribution (*3*). Therefore, GL113 or RB6-8C5 treated animals exposed to infected sand fly bites were compared using an exact stratified Wilcoxon rank sum test, stratified by experiment in order to allow pooling of experiments as described in the text. The odds ratios across experiments to determine the likelihood of the presence of infection in GL113 or RB6-8C5 treated animals following exposure to infected sand fly bite was calculated using the conditional maximum likelihood estimate with exact confidence interval after checking the homogeneity assumption of odds ratios among experiments by Zelen's exact test (see e.g., Cytel StatXact 8 Procs Manual). All p-values are two-sided. Both the stratified Wilcoxon and the odds ratio calculations were done in StatXact 8 Procs (Cytel, Inc., Cambridge, MA).

Supplemental Figures

Figure S1.

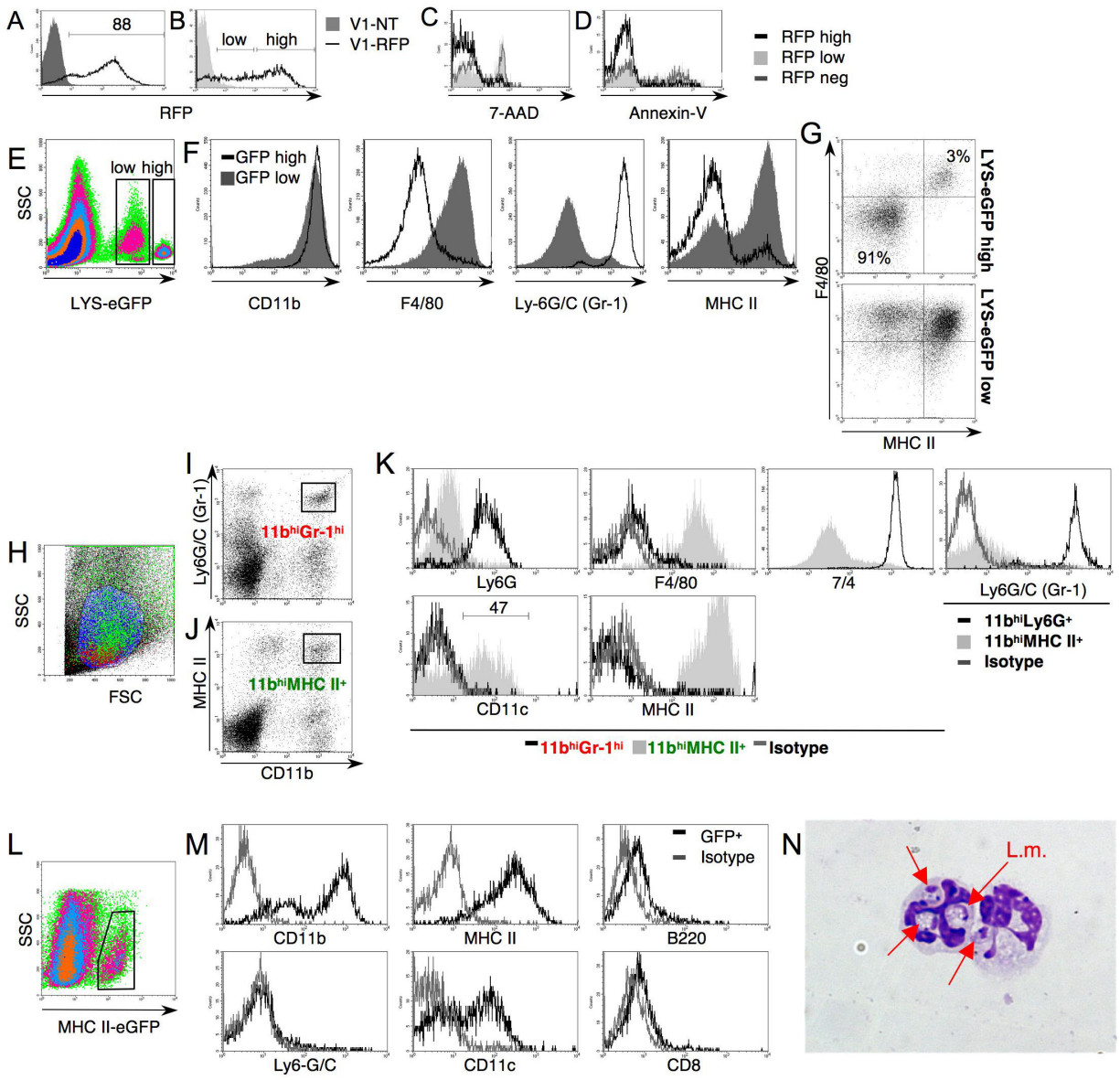

Figure S1. Phenotypic Analysis of *L. major*-RFP and murine ear cells derived from mice used in this study following infection with *L. major*-RFP. (A) RFP expression of the *L. major*-RFP parasite employed in this study following metacyclic promastigote purification of a day 4 culture. **(B-D)** Comparison of 7-AAD staining (C),

and AnxA5 binding (D), among parasites with different levels of RFP expression as shown in (B). **(E-G)** Phenotypic analysis of cells derived from LYS-eGFP mice 90" p.i. with 10^6 *L. major* parasites. **(E)** SSC/eGFP dot plot of ear cells. Gates indicate $eGFP^{hi}$ and $eGFP^{low}$ expressing cells. **(F)** Phenotypic histogram analysis of LYS-$eGFP^{hi}$ and LYS-$eGFP^{lo}$ cells from (E). **(G)** Staining for $F4/80^+MHCII^-$ monocytes among GFP^{hi} and GFP^{low} cells reveals that these cells reside in the GFP^{low} population and that GFP^{hi} neutrophils are distinct from $CX3CR1^+F4/80^+$monocytes that are recruited into the skin in response to inflammatory stimuli (*7, 8*). **(H-K)** Phenotypic analysis of cells derived from C57BL/6 mice 2 hours post infection with 10^6 wt *L. major* parasites. **(H)** FSC/SSC plot of ear cells, $CD11b^+Gr\text{-}1^{hi}$ cells (defined as neutrophils based on this phenotype as well as subsequent staining as indicated in K) are highlighted red and $CD11b^+MHCII^+$ cells are highlighted green. $CD11b^+F4/80^+$ cells were defined as macrophages/monocytes and contain both $MHCII^+$ and $MHCII^-$ cells. Blue highlight indicates the R1 gate at this time point. It should be noted that neutrophils derived from the ear dermis have a SSC/FSC profile that is distinct from that of neutrophils isolated from the blood (data not shown). **(I)** CD11b/Ly6-G/C(Gr-1) and **(J)** CD11b/MHC II dot plot of SSC/FSC R1 gated ear cells. **(K)** Phenotypic histogram analysis of $CD11b^+$/Ly6-$G/C(Gr\text{-}1)^+$, $CD11b^+Ly6\text{-}G^+$ and $CD11b^+$MHC II^+ cells. **(L and M)** Phenotypic analysis of cells derived from MHC II-eGFP mice 2 hours post infection with 10^6 wt *L. major* parasites. **(L)** SSC/eGFP dot plot of ear cells. **(M)** Phenotypic histogram analysis of MHC II-$eGFP^+$ cells gated as shown in (L). **(N)** Representative example of infected neutrophils following cytospin of LYS-eGFP ear preparations 12 hours following infection with $1x10^6$ *L. major*-RFP. Similar results were found following infection of wt

C57BL/6 mice (data not shown). Analysis of cytospin preparations of ear tissue demonstrated that of the total number of intracellular parasites counted 12 hours post-infection (p.i.), 69% (+/- SD 4, n=3 experiments) were inside cells with polymorphic nuclei.

Figure S2.

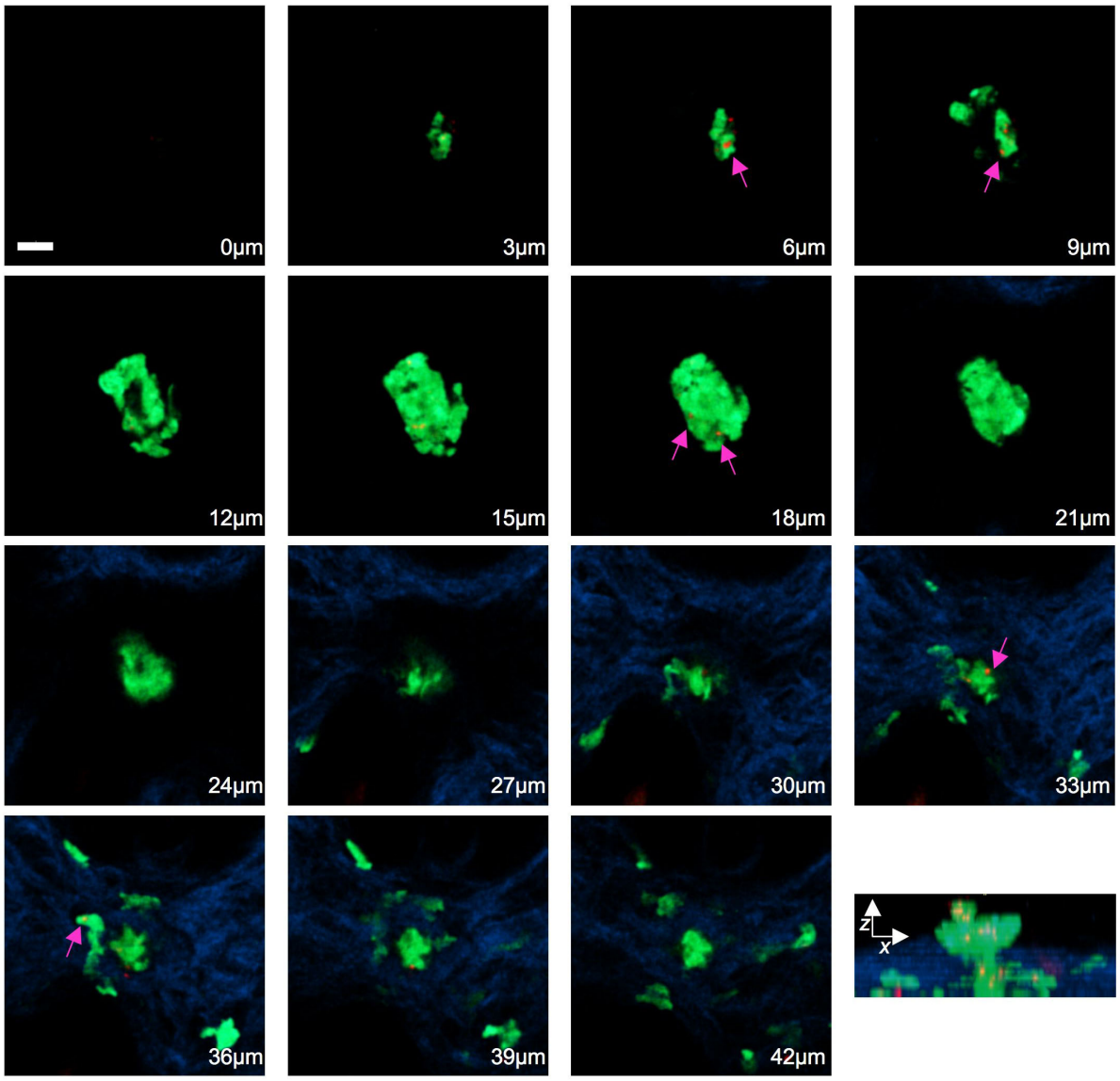

Figure S2. Phagocytosed parasites can be found in neutrophil "plugs" following bites with infected sand flies. 3-dimensional image series derived from a 2P-IVM data set of the ear of a LYS-eGFP mouse (green) 2 hours after being bitten with *L. major*-RFP (red)-infected sand flies. The second harmonic signal (blue) allows identification of the dermis. Depth from the surface of the skin is shown. The final panel is a maximum intensity projection image across the Y dimension. Arrows point to parasites inside of neutrophils. Scale bar, 15µm.

Figure S3.

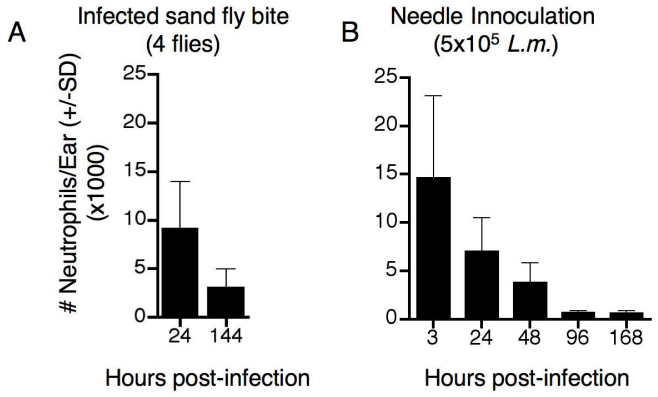

Figure S3. Analysis of the inflammatory response to needle inoculation versus infected sand fly bite reveals a comparable early recruitment of neutrophils but that only sand fly bite maintains neutrophils at the site. (A and B) Total number of neutrophils per ear at various times following exposure to 4 infected *P. duboscqi* sand flies for 3 hours (A) or needle inoculation of $5x10^5$ *L. major* metacyclic promastigotes in 10μl (B).

Figure S4.

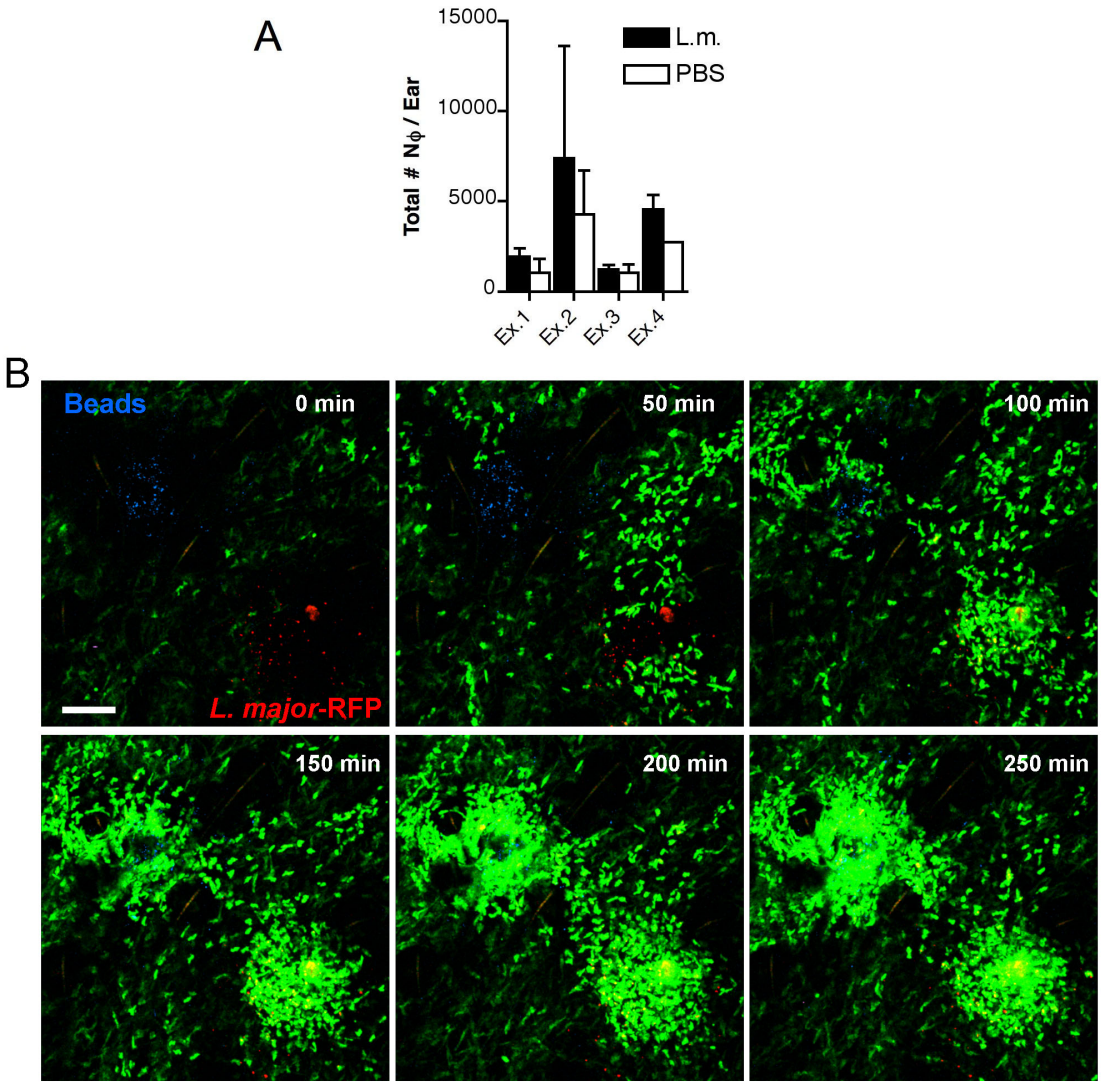

Figure S4. Neutrophils recruitment into the ear following i.d. inoculation is independent of parasite. (A) Flow analysis of neutrophil recruitment 90" following needle inoculation of PBS versus $1x10^6$ (Ex.1-3) or $7x10^5$ (Ex.4) *L. major* in a volume of 10μl (Ex.1 and 2), 5μl (Ex.4), or 2μl (Ex.3) in four separate experiments, n=2-4 ears per group. **(B)** 2P-IVM time-lapse image series from the ear of a LYS-eGFP mouse (green) beginning 30" after inoculation with fluorescent beads (blue) in the upper left quadrant of the imaging frame and *L. major*-RFP (red) in the lower right quadrant of the imaging

frame. Individual solutions of beads and parasite were placed adjacent to one another on the surface of the skin in a 1µl volume and a single needle stick through each solution into the dermis was used to deposit the particles. Scale bar, 100µm. See also movie S9.

Figure S5.

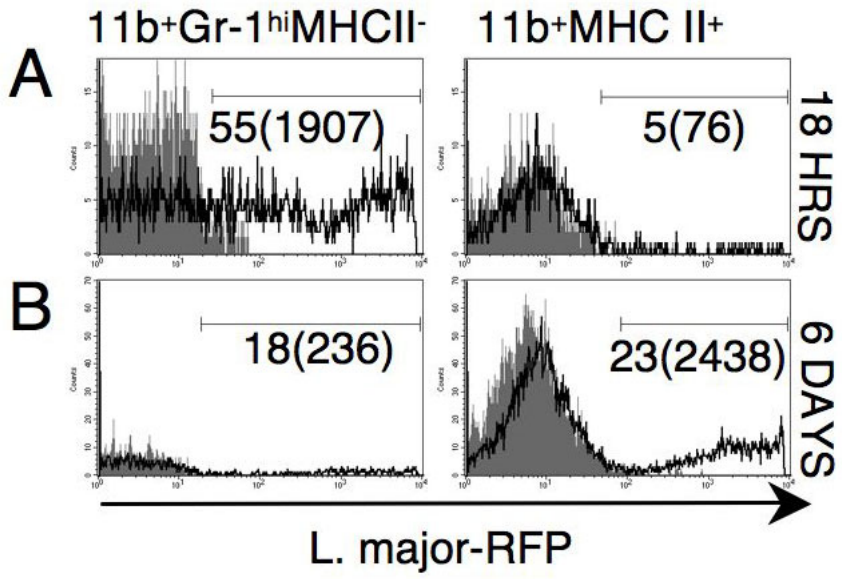

Figure S5. Histogram analysis of RFP expression among neutrophils (CD11b^{+}Gr-1^{hi}MHC II-eGFP^{-}) and macrophages/monocytes (CD11b^{+}MHCII-GFP^{+}) (A) Cell number/RFP histogram of the indicated populations from ears of MHC II-eGFP mice at 18 hours (A) and 6 days (B) post-infection with 1x10^{6} *L. major*-RFP. Numbers outside of parentheses represent the frequency of gated cells expressing an RFP signal, numbers inside parentheses indicate total number of cells/sample.

Figure S6.

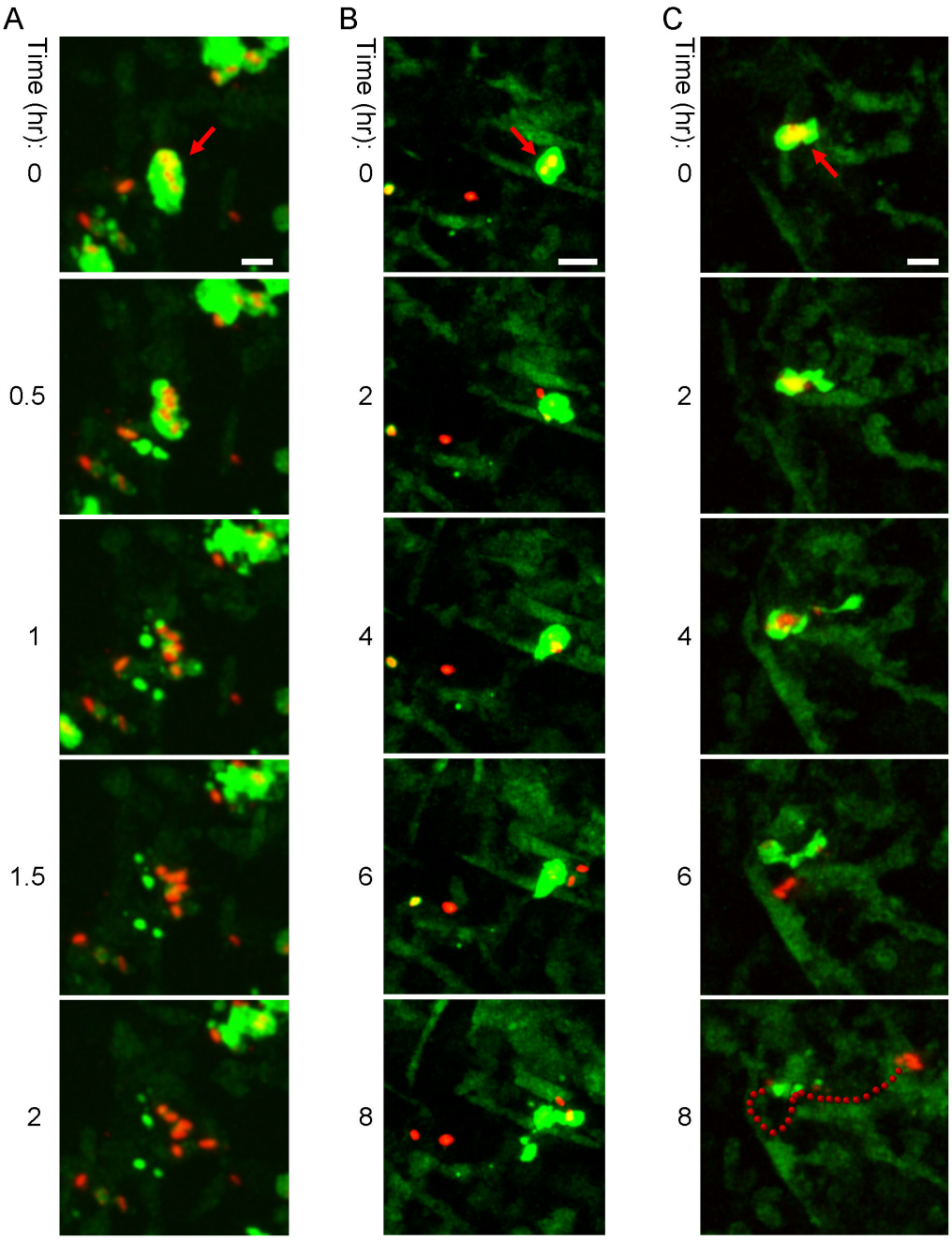

Figure S6. Three examples of parasites being released from infected neutrophils shortly before or during apoptosis. Images represent maximum intensity projections derived from 4-dimensional data sets of CSF1R-eGFP mice that had been bitten with uninfected sand flies 12 hours earlier to induce inflammation and subsequently

inoculated with $1x10^4$ *L. major*-RFP containing neutrophils sorted from the ears of infected LYS-eGFP mice (see Figure 4). eGFP-expressing cells are shown in green ($eGFP^{hi}$= LYS-eGFP neutrophils, $eGFP^{low}$= CSF1R-eGFP macrophage/monocytes) and *L. major* is shown in red. Final image in C shows path of parasites following release from an apoptotic neutrophil and apparent uptake by a non-fluorescent host cell. For all data sets, parasite fluorescence was completely contained within LYS-eGFP fluorescence in 3-dimensional space at the beginning of the image series. Scale bar, 10μm. See also movies S10, S11, and S12.

Figure S7.

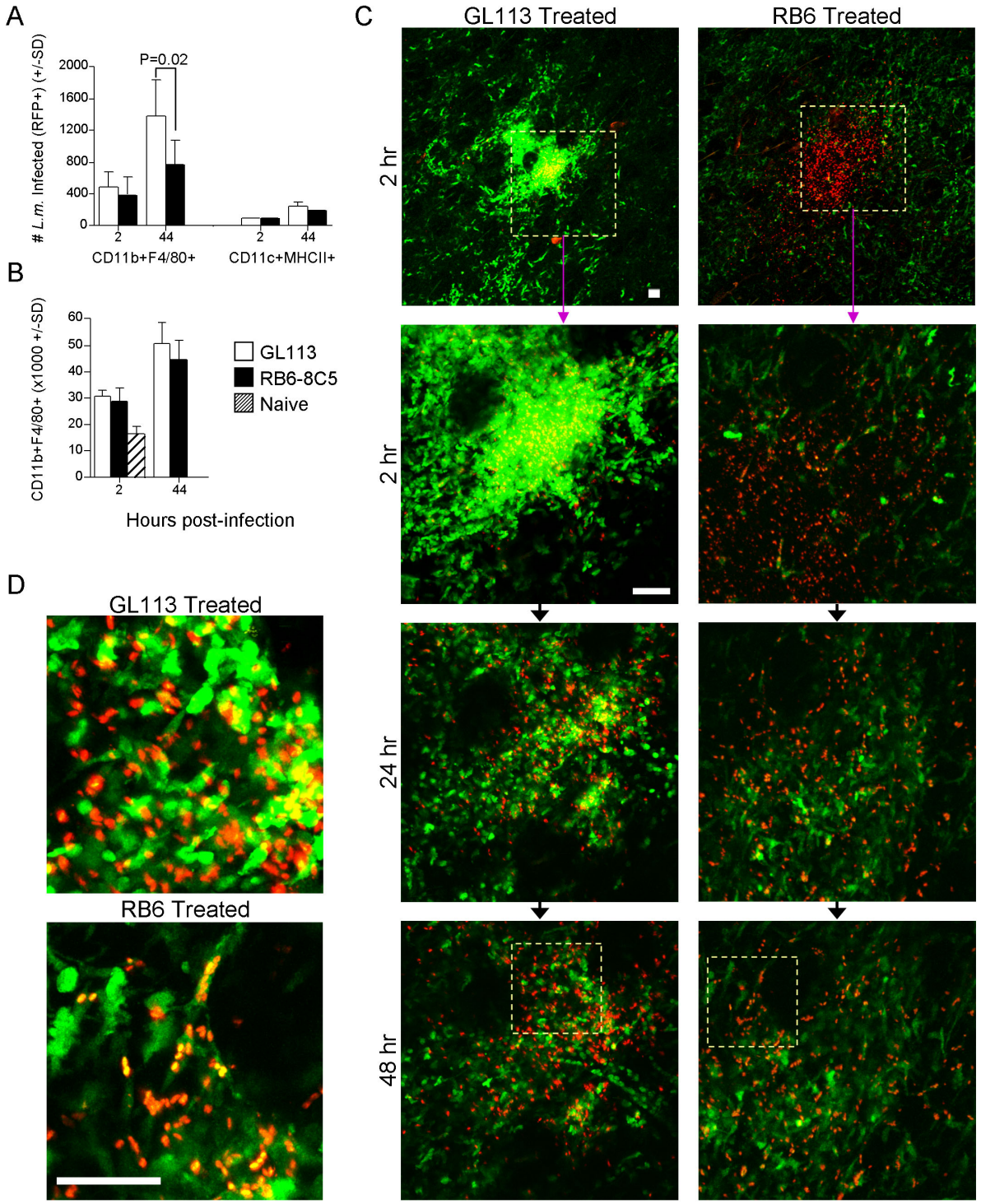

Figure S7. The host response to needle inoculation of parasites in the absence of neutrophils. (A-B) Recruitment and infection of phagocytic cells at sites of parasite deposition in the presence or absence of neutrophils. The number of infected (R2 gated

as shown in Fig. 2C) $RFP^+CD11b^+F4/80^+$ macrophage/monocytes or $RFP^+CD11c^+MHCII^+$ Langerhans/dendritic cells (A), and the total number of $CD11b^+F4/80^+$ macrophage/monocytes (B) per ear (+/- SD n=4-6 ears/group/time point), was assessed at 2 and 44 hours following inoculation of control (GL113-treated) or neutrophil-depleted (RB6-8C5-treated) C57BL/6 mice with $1x10^5$ *L.m.*-RFP in 2ul PBS. The number of cells in a naïve ear is shown for the 2-hour time point. Data are representative of 2 independent experiments. **(C)** Migration of LYS-$eGFP^+$ cells to sites of parasite deposition in the presence and absence of neutrophils. Control or neutrophil-depleted LYS-eGFP animals were inoculated with $1x10^4$ *L.m.*-RFP and examined 2, 24 and 48 hours later. The top panel of images represents a low magnification view of the infection site with the boxed region indicating the area represented in the remaining images of the time series. **(D)** Magnified views of the boxed regions from the 48 hour time point in part B. All images were obtained by repeatedly imaging the same site infection from the ears of the same two mice (GL113 and RB6-8C5-treated) at the indicated time points. Identical regions of skin were identified on different days based on patterns of parasite deposition, the surrounding hair follicles, and blood vasculature. Images are representative of data obtained from 4 animals per group captured from 2 independent experiments. Scale bars; 50μm.

Supplemental References

1. N. Faust, F. Varas, L. M. Kelly, S. Heck, T. Graf, *Blood* **96**, 719 (2000).
2. M. Boes *et al.*, *Nature* **418**, 983 (2002).
3. N. Kimblin, Peters, N., Debrabant, A., Secundino, N., Egen, J., Lawyer, P., Fay, M.P., Kamhawi, S., Sacks, D., *PNAS,* In press.
4. Y. Belkaid, H. Jouin, G. Milon, *Journal of Immunological Methods* **199**, 5 (1996).
5. H. Qi, J. G. Egen, A. Y. C. Huang, R. N. Germain, *Science* **312**, 1672 (2006, 2006).
6. Y. Belkaid *et al.*, *J Immunol* **165**, 969 (2000).
7. C. Auffray *et al.*, *Science* **317**, 666 (2007).
8. R. T. Palframan *et al.*, *J Exp Med* **194**, 1361 (2001).